

LS-DYNA Simulation of Hemispherical-punch Stamping Process Using an Efficient Algorithm for Continuum Damage Based Elastoplastic Constitutive Equation

Nima Salajegheh*, Nader Abedrabbo and Farhang Pourboghrat

Department of Mechanical Engineering, Michigan State University, East Lansing, MI 48824-1226

Abstract. An efficient integration algorithm for continuum damage based elastoplastic constitutive equations is implemented in LS-DYNA. The isotropic damage parameter is defined as the ratio of the damaged surface area over the total cross section area of the representative volume element. This parameter is incorporated into the integration algorithm as an internal variable. The developed damage model is then implemented in the FEM code LS-DYNA as user material subroutine (UMAT). Pure stretch experiments of a hemispherical punch are carried out for copper sheets and the results are compared against the predictions of the implemented damage model. Evaluation of damage parameters is carried out and the optimized values that correctly predicted the failure in the sheet are reported. Prediction of failure in the numerical analysis is performed through element deletion using the critical damage value. The set of failure parameters which accurately predict the failure behavior in copper sheets compared to experimental data is reported as well.

INTRODUCTION

Application of fracture mechanics to characterize ductile fracture has led to the introduction of different ductile fracture criteria, which notably include J-integral. These criteria offer a tool for predicting the crack propagation at the macroscale but they fail to take into account the continuous deterioration of material properties as the effect of microcrack nucleation and accumulation. Moreover, fracture mechanics deals with the analysis of existing cracks which might not be present or exactly located. Forming limit diagrams, on the other hand, have proved to be reliable for predicating the initiations of material discontinuities, however, FLD's also neglect the material softening behavior resulting from continuous material deterioration. Hence, the concept of continuum damage mechanics has gained credit for taking into account the continuous deterioration of material and predicting failure.

The idea was introduced when in 1958 L. M. Kachanov [1] published a simple model of material damage for creep analysis. Ever since, the concept has been expanded through excellent work of researchers

such as D. Krajcinovic et al [2, 3], F. A. Leckie et al [4], J. L. Chaboche et al [5], S. Murakami et al [6], C. L. Chow et al [7-11], J. Lemaitre et al [12-17] and other fine researchers to the point of application to real-life problems.

Damage Parameter, Effective Stress, and the Equivalence Principle

Damage may be in the form of creation of discontinuous surfaces, breaking of atomic bonds, or growth of microcavities. Following the work of L. M. Kachanov [1], at the mesoscale, damage may be approximated in any plane by the area of the intersections of all the flaws with that plane. In order to work with a dimensionless quantity, this area is scaled by the size of the representative volume element (RVE). For a RVE oriented along the direction \vec{n} , we can define δS as the area of the section of the RVE and δS_D as the area of the intersections of all microcracks or microcavities which lie in δS as seen in Figure 1.

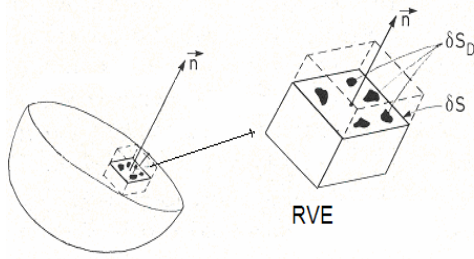


FIGURE 1. Isotropic definition of damage parameter [1].

The value of the damage at point M in the direction \vec{n} is defined as:

$$D(M, \vec{n}) = \frac{\delta S_D}{\delta S} \quad (1)$$

The scalar (isotropic) damage parameter at point M is the maximum value of $D(M, \vec{n})$ for all possible orientations of \vec{n} . It follows from this definition that the value of the scalar variable D is bounded by 0 and 1 as follows:

$$\begin{aligned} D = 0 &\rightarrow \text{Undamaged material} \\ D = 1 &\rightarrow \text{Fully broken material} \end{aligned} \quad (2)$$

In fact, the failure occurs for $D < 1$ through a process of instability. Since no force is carried by the broken area represented by S_D , an effective stress, $\tilde{\sigma}$, can be introduced which is based on the surface that effectively resists the load, namely $(S - S_D)$:

$$\tilde{\sigma} = \frac{F}{S - S_D} = \frac{F}{S \left(1 - \frac{S_D}{S}\right)} = \frac{\sigma}{1 - D} \quad (3)$$

In compression, some defects close and the surface that effectively resists the load becomes larger than $(S - S_D)$. In particular, if all the defects close, the effective stress in compression is equal to the usual stress. Moreover, the damage evolution is almost zero and the damage parameter remains constant. This effect is called the ‘‘crack closure effect’’ and is taken into account, in this work, by introducing a factor in the numerical implementation of damage evolution equation. When the material is in compression, negative hydrostatic pressure, the factor is set equal to zero and is set equal to one for positive values of hydrostatic stress. However, since the damage evolution in compression may not be negligible for some materials and temperatures, one can introduce a

material parameter ranging from zero to one which could be determined experimentally.

To include the damage parameter into the constitutive equations, different criteria have been postulated [10]. In this work, the Strain Equivalence Principle introduced by Lemaitre [13] has been utilized. This principle states that any strain constitutive equation for a damaged material may be derived in the same way as for a virgin material except that the usual stress is replaced by the effective stress:

$$\begin{aligned} \varepsilon(\sigma, D) &= \varepsilon(\sigma, 0) \\ \tilde{\sigma} &= \frac{\sigma}{1 - D} \end{aligned} \quad (4)$$

Damage Evolution Equation and the Computational Algorithm

Assuming an isotropic power law hardening rule, Lemaitre postulated the damage evolution equation to be [12]:

$$\sigma_y = K(\varepsilon_0 + p)^n \quad (5)$$

$$\begin{aligned} \dot{D} &= \left(\frac{D_c}{\varepsilon_{PR} - \varepsilon_{PD}} \right) \times \\ &\left[\frac{2}{3}(1 + \nu) + 3(1 - 2\nu) \left(\frac{\sigma_H}{\sigma_{eq}} \right)^2 \right] (\varepsilon_0 + p)^{2n} \dot{P} \end{aligned} \quad (6)$$

Where ε_{PD} is the plastic strain below which the damage evolution is negligible. ε_{PR} is the plastic strain at rupture. D_c is the damage parameter at rupture called the critical value of damage. σ_H is the hydrostatic stress. σ_{eq} is the von Mises equivalent stress. σ_y is the yield stress. ε_0 is the strain value at yield. K and n are isotropic hardening coefficients. p is the equivalent plastic strain which is written as:

$$p = \sqrt{\frac{2}{3} \varepsilon^p : \varepsilon^p} \quad (7)$$

Applying the strain equivalence principle, yielding occurs when:

$$\tilde{\sigma} = \frac{\sigma}{1 - D} = \sigma_y = K(\varepsilon_0 + p)^n \quad (8)$$

Thus, the von Mises yield function may be written in the following form:

$$f(\sigma^D) = \frac{3}{2} \sigma^D : \sigma^D - (1-D)^2 \sigma_y^2 \leq 0 \quad (9)$$

Where σ^D is the deviatoric stress tensor. The radius of yield function and the normal unit vector are:

$$R = \sqrt{\frac{2}{3}} (1-D) \sigma_y \quad (10)$$

$$N = \frac{\sigma^D}{|\sigma^D|} = \frac{\sigma^D}{\sqrt{\sigma^D : \sigma^D}} = \frac{\sigma^D}{R} = \sqrt{\frac{3}{2}} \frac{\sigma^D}{(1-D) \sigma_y} \quad (11)$$

Assuming that the total strain rate is the summation of the elastic and plastic parts, $\dot{\varepsilon} = \dot{\varepsilon}^e + \dot{\varepsilon}^p$, and applying the flow rule to the plastic part, $\dot{\varepsilon}^p = \dot{\gamma} N$, the equivalent plastic strain rate can be written as:

$$\dot{p} = \sqrt{\frac{2}{3} \dot{\varepsilon}^p : \dot{\varepsilon}^p} = \sqrt{\frac{2}{3}} \dot{\gamma} \quad (12)$$

Other equations used in the implementation of the computational algorithm are as follows:

Stress rate:

$$\dot{\sigma} = (1-D) (\lambda \text{trace}(\dot{\varepsilon}^e) I + 2\mu \dot{\varepsilon}^e) \quad (13)$$

Equivalent von Mises stress:

$$\sigma_{eq} = \sqrt{\frac{3}{2} \sigma^D : \sigma^D} \quad (14)$$

Isotropic hardening law:

$$h = nK (\varepsilon_0 + p)^{n-1} \quad (15)$$

The computational algorithm aims at calculating the stress, strain, and damage parameters at the end of a small time (strain) increment given their values at the beginning of the increment and the components of total strain tensor applied over the increment.

First, the increment is assumed to be totally elastic and the elastic predictor is calculated as the trial stress for the new increment:

$$\sigma_{new}^{trial} = \sigma_{old} + (1-D_{old}) (\lambda \text{trace}(\Delta \varepsilon) I + \mu \Delta \varepsilon) \quad (16)$$

If the elastic predictor, σ_{new}^{trial} , is within the current yield surface, the elastic predictor is the actual value of stress for the current increment:

$$\sigma_{new} = \sigma_{new}^{trial} \quad (17)$$

If not, a plastic correction should be made as following:

$$\begin{aligned} \sigma_{new} &= \sigma_{new}^{trial} - 2\mu \Delta \varepsilon^p (1-D_{old}) = \\ &\sigma_{new}^{trial} - 2\mu \Delta \gamma N (1-D_{old}) \end{aligned} \quad (18)$$

We seek to find $\Delta \gamma$. Since the increment is no longer totally elastic, the value of total equivalent plastic strain, p , needs to be updated:

$$p_{new} = p_{old} + \sqrt{\frac{2}{3}} \Delta \gamma \quad (19)$$

And the new yield stress considering the plastic hardening is calculated as:

$$\begin{aligned} \sigma_{y_{new}} &= \sigma_{y_{old}} + h \Delta p = \\ &\sigma_{y_{old}} + nK (\varepsilon_0 + p)^{n-1} \sqrt{\frac{2}{3}} \Delta \gamma \end{aligned} \quad (20)$$

If $p \geq \varepsilon_{pD}$, the damage parameter has to be updated using the Lemaitre's equation:

$$\begin{aligned} D_{new} &= D_{old} + \Delta D \\ \Delta D &= \left(\frac{D_c}{\varepsilon_{PR} - \varepsilon_{PD}} \right) \times (\varepsilon_0 + p)^{2n} \sqrt{\frac{2}{3}} \Delta \gamma \\ &\left[\frac{2}{3} (1+\nu) + 3(1-2\nu) \left(\frac{\sigma_H}{\sigma_{eq}} \right)^2 \right] \end{aligned} \quad (21)$$

Then, $\Delta \gamma$ is determined considering constant D during one step which is justified in the explicit calculation because of very small increments. At the end of increment:

$$\begin{aligned} \sigma_{y_{new}} &= \sigma_{y_{old}} + h \Delta p = \\ &\sigma_{y_{old}} + nK (\varepsilon_0 + p)^{n-1} \sqrt{\frac{2}{3}} \Delta \gamma \end{aligned} \quad (22)$$

$$\begin{aligned} \sigma_{new}^D &= R_{new} N = \sqrt{\frac{2}{3}} (1-D_{old}) \sigma_{y_{new}} N \\ \sigma_{new}^{D_{trial}} - 2\mu\Delta\gamma(1-D_{old})N &= \sqrt{\frac{2}{3}} (1-D_{old}) \left(\sigma_{y_{old}} + \sqrt{\frac{2}{3}} h\Delta\gamma \right) N \\ \sigma_{new}^{D_{trial}} &= \left\{ \sqrt{\frac{2}{3}} \left(\sigma_{y_{old}} + \sqrt{\frac{2}{3}} h\Delta\gamma \right) + 2\mu\Delta\gamma \right\} (1-D_{old}) N \\ &= \left\{ \sqrt{\frac{2}{3}} \sigma_{y_{old}} + \left(\frac{2}{3} h + 2\mu \right) \Delta\gamma \right\} (1-D_{old}) N \\ \sqrt{\sigma_{new}^{D_{trial}} : \sigma_{new}^{D_{trial}}} &= (1-D_{old}) \left\{ \sqrt{\frac{2}{3}} \sigma_{y_{old}} + \left(\frac{2}{3} h + 2\mu \right) \Delta\gamma \right\} \\ \therefore \Delta\gamma &= \frac{\left\{ \sqrt{\sigma_{new}^{D_{trial}} : \sigma_{new}^{D_{trial}}} - \sqrt{\frac{2}{3}} (1-D_{old}) \sigma_{y_{old}} \right\}}{2\mu \left(1 + \frac{h}{3\mu} \right) (1-D_{old})} \end{aligned} \quad (23)$$

Hemispherical-Punch Stamping Experiment

The experiments were performed using a 1.6 mm thick copper 99.9% sheet cut into a 179 mm square blank. The blank was then clamped between the die and the holder; the punch then moves upward and deforms the sheet into a hemispherical-shape cup. Figure 2 shows a schematic illustration of the setup. For material characterization, several uniaxial tensile tests were performed based on ASTM E8M standard and the results were averaged to obtain the mechanical properties of the material as reported in table 1.

TABLE 1. Material properties

Property	Magnitude
Young's modulus	98.99 GPa
Poisson's ratio	0.34
Yield stress	90.0 MPa
K (Hardening coefficient)	491.3 MPa
n (Hardening exponent)	0.2459

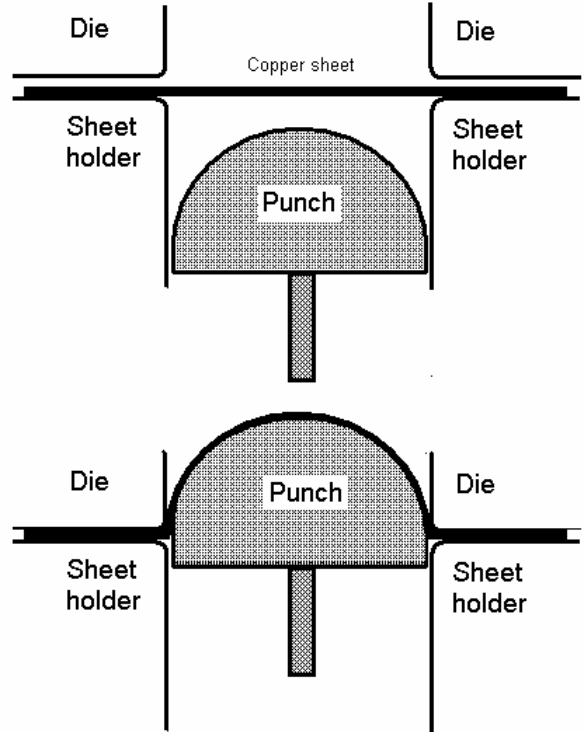


Figure 2. Beginning and the end of the stamping process

Numerical Results

The computational algorithm is implemented into the nonlinear finite element code, LS-DYNA through the user material subroutine option, UMAT. The material model is then used in the simulation of a hemispherical-punch stamping process. The numerical model used in the simulation is shown in Figure 3.

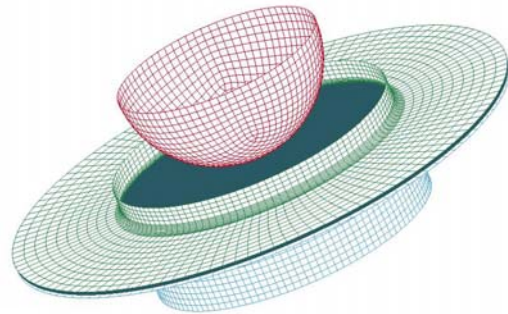


Figure 3. Numerical model used in FEM simulation.

The punch, die, and blank holder were meshed with rigid elements. 76300 hexagonal quadratic solid elements were used to mesh the sheet part. Two cases were studied which differed in the material damage parameters. In case 1, these parameters were taken from the literature [14]; and in case 2, they were optimized and suggested by the authors after a series of sensitivity analysis. The values are listed in table 2.

TABLE 2. Material damage parameters

Parameter	Case 1	Case 2
\mathcal{E}_{PD}	0.35	0.33
\mathcal{E}_{PR}	1.07	0.48
D_c	0.85	0.68

Monitoring the punch force variations is a good way to see the softening behavior of material as the damage grows. Figure 4 shows a comparison of punch force vs. punch displacement between both cases of study compared against experimental results.

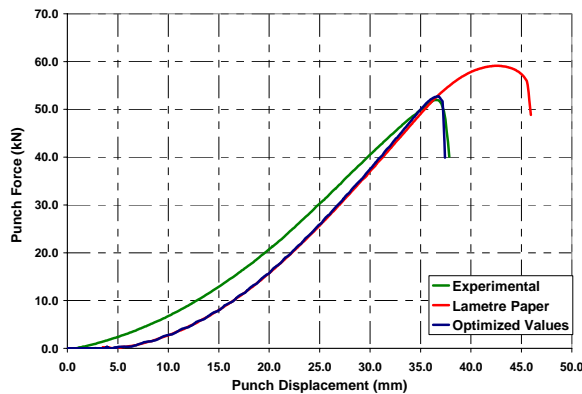


Figure 4. Comparison of punch force vs. its displacement between numerical and experimental findings

In the analysis, failure was predicted using the critical value of damage and demonstrated by element deletion method which was implemented into the UMAT.

Figure 5 shows a picture of the experimental result of forming of the copper sheet. Figure 6 shows a picture of the numerical analysis using the optimized damage values as reported in Table 2.

As seen from Figure 4, the damage parameters reported in literature [14] for the pure copper used in this experiment were unable to predict the behavior seen experimentally. The optimized values of damage, on the other hand, were capable of predicting both failure locations (Figure 5 and Figure 6) and the punch force (Figure 4).



Figure 5. Experimental result of forming of 99.9% copper sheet.

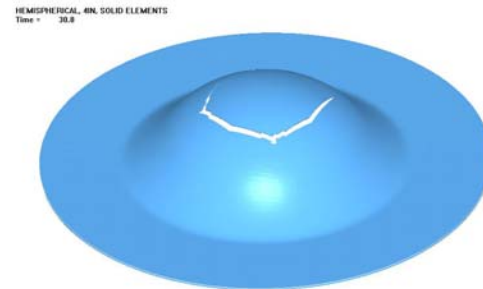


Figure 6. Comparison of failure between numerical and experimental findings

Conclusions

The softening behavior of material and its effect on the punch force was satisfactorily captured by using a continuum damage based material model with optimized damage parameters. The material model proved to be particularly functional in predicting failure location compared to experimental results. Nevertheless, mesh dependency and the assumption of zero damage growth in compression are two limitations which should be carefully dealt with when the material model is to be used for the simulation of other forming processes with different loading conditions.

ACKNOWLEDGMENTS

The first author would like to acknowledge and thank Dr. Sang-Wook Lee, assistant professor in the department of Mechanical Engineering at Soonchunhyang University in Korea, for his contribution for the derivation of the numerical algorithm.

REFERENCES

1. Kachanov, L.M., Introduction to continuum damage mechanics, Dordrecht, Boston: Martinus Nijhoff Publishers, 1986.
2. Krajcinovic, D., and Fonseka, G.U., Journal of Applied Mechanics, 48, 809-824 (1981).
3. Krajcinovic, D., Journal of Applied Mechanics, 52, 829-834 (1985).
4. Onat, E.T., and Leckie, F.A., Journal of Applied Mechanics, 55, 1-10 (1988).
5. Chaboche, J.L., Nuclear Engineering and Design, 79, 309-319 (1984).
6. Murakami, S., Journal of Applied Mechanics, 55, 280-286 (1988).
7. Chow, C.L., and Wang, J., International Journal of Fracture, 33, 3-16 (1987).
8. Chow, C.L., and Wang, J., Engineering Fracture Mechanics, 27, 547-558 (1987).
9. Chow, C.L., and Lu, T.J., Engineering Fracture Mechanics, 34, 679-701 (1989).
10. Chow, C.L., and Wang, J., Engineering Fracture Mechanics, 30, 547-563 (1988).
11. Chow, C.L., and Wang, J., International Journal of Fracture, 38, 83-102 (1988).
12. Lemaitre, J., Journal of Engineering Materials and Technology, 107, 83-89 (1985).
13. Lemaitre, J., A Course on Damage Mechanics, New York: Springer, 1996.
14. Lemaitre, J., and Chaboche, J.L., Mechanics of Solid Materials, Cambridge: Cambridge University Press, 1990.
15. Lemaitre, J., and Doghri, I., Computer methods in applied mechanics and engineering, 115, 197-232 (1994).
16. Lemaitre, J., and Dufailly, J., Engineering Fracture Mechanics, 28, 643-661 (1987).
17. Lemaitre, J., and Desmorat, R., and Sauzay, M., European Journal of Mechanics - A/Solids, 19, 187-208 (2000).